Available online at www.sciencedirect.com

ScienceDirect

Procedia Engineering 109 (2015) 43 – 54

Procedia Engineering

www.elsevier.com/locate/procedia

XXIII Italian Group of Fracture Meeting, IGFXXIII

# Pipeline corrosion failure in an absorption chiller

Andrea Brotzu*, Ferdinando Felli, Stefano Natali, Daniela Pilone

*Dip. ICMA, Sapienza Università di Roma, Via Eudossiana 18, 00184 Roma, Italy*

**Abstract**

Absorption chillers generate chilled water by employing as refrigerant water which is evaporated at low pressure. The steam produced is then absorbed by a concentrated LiBr solution. The materials employed for the construction of this kind of plant are usually copper and stainless steel. Despite their good corrosion resistance, the environment rich of halogen ions can lead in some cases to severe corrosion attacks.

This paper describes a complex case of corrosion that produced the failure of an absorption chiller pipelines. The failure involved in different steps both copper and stainless steel pipes.



Peer-review under responsibility of the Gruppo Italiano Frattura (IGF)

*Keywords:* Absorption chiller; localized corrosion; LiBr solution.

## 1. Introduction

This paper describes a complex case of corrosion failure that occurred in the pipelines of an absorption chiller. The absorption chillers produce chilled water up to 4.5 °C and are characterized by an absorption cycle using water/lithium bromide as working fluid. Unlike a compression chiller which uses a compressor to pressurize the vaporized refrigerant (Freon) and condenses it by using cooling water, the absorption chiller uses an absorbent (LiBr) to absorb the vaporized refrigerant (water). The refrigerant is then released from the absorbent when heated by an external source.

The absorption chillers utilize for cooling the latent heat released by the refrigerant (water) when it evaporates in a closed vessel. Fig. 1 shows the schema of this kind of plant.

The water that has to be chilled flows into a pipeline present in the evaporator which is maintained at a very low pressure (usually 6 mm Hg). Water (refrigerant) passes over these pipes and, being the pressure in the absorber-

* Corresponding author. Tel.: +39.0644585550.
*E-mail address:* andrea.brotzu@uniroma1.it


Peer-review under responsibility of the Gruppo Italiano Frattura (IGF)
doi:10.1016/j.proeng.2015.06.205

evaporator shell very low, the water boils at a very low temperature. This boiling determines heat absorption from the pipeline, thus lowering the temperature of the water to be cooled.

The evaporated water passes in the absorber section of the chiller where it is mixed with a concentrated solution of lithium bromide. This solution absorbs the water vapor, becomes more diluted and rapidly loses its capability to absorb water vapor. The weak lithium bromide solution is then pumped to the generator section where it is heated by an external source. The evaporated water is recovered in a condenser and reused as refrigerant to repeat the cycle.

In order to increase heat transfer efficiency, usually this kind of chiller is equipped with copper or copper alloy pipes. On the other hand stainless steel is used for other components like generator and vessel.

One of the primary issues concerning absorption chillers is the selection of the materials that can be used in the different sections of the plant. In fact lithium bromide solution produces an aggressive environment. Corrosion phenomena may be exacerbated by different factors such as temperature and high halogen concentration. Different type of corrosion attacks can occur in this kind of plant. For example the coupling between different materials (i.e copper tube - steel flanges) can produce galvanic corrosion. Moreover the temperature of the LiBr solution changes in different sections of the absorption system and hence thermogalvanic corrosion might also occur. These units operate under flowing conditions and the effect of fluid flow has been considered as one of the major problems because it can increase corrosion rates. Moreover halide ions usually are responsible for the destabilization of the passive film that protects copper and stainless steel surfaces and then their presence can determine localized corrosion phenomena such as crevice corrosion (i.e. between tube and support septa) or pitting.

The corrosion behavior of materials in solutions containing chloride ions has been deeply studied, but only a limited number of papers concerning the behavior of metallic materials in lithium bromide solutions can be found in literature.

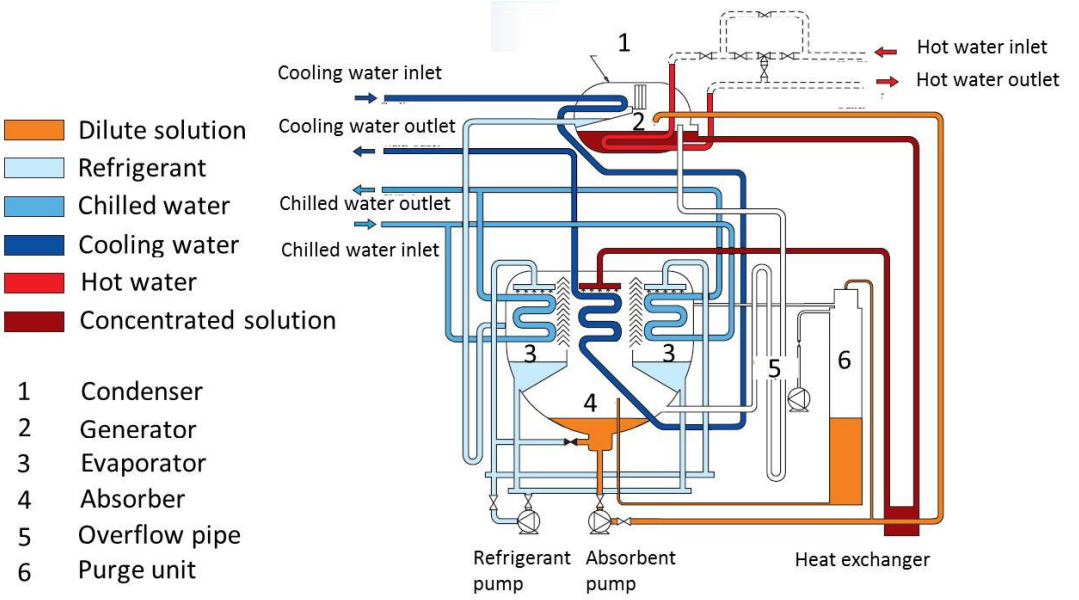


Fig. 1. Scheme of an absorption chiller.

## 2. Materials and failure description

The pipelines of the failed absorption chiller were made of copper and stainless steel. Table 1 reports the kind of tubes employed in different plant sections and the different fluids that were in contact with them.

Table 1. Pipes materials and fluid description

| Plant zones | Kind of tube | Internal fluid | External fluid |
|---|---|---|---|
| Condenser | Copper plain tube | Refrigerant | Cooling water |
| Absorber | Copper Minifinned (externally) tubes | Cooling water | LiBr solution |
| Evaporator | Copper corrugated tubes | Chilled water | Refrigerant (distilled water) |
| Generator | Stainless steel Minifinned (externally) tubes | Hot water | LiBr solution |

EDS analyses carried out on copper tubes show that they are made of pure copper (no alloying elements have been identified).

Analyses carried on stainless steel components by means of a spectrometer highlighted the composition reported in Table 2; this composition confirmed the analyses initially performed by EDS (Fig. 2). A bare observation of steel pipes revealed that there is a clearly visible axial welding seam along the whole tube that indicates that this is a calendared tube. Titanium stabilized stainless steel has been selected in order to avoid sensitization phenomena during welding. Fig. 3 shows the microstructure of this alloy. The microstructure is characterized by fine equiaxed grains and by the presence of a fine dispersion of bright particles . EDS analysis revealed that they are titanium carbide/nitride particles (Fig. 4).

As far as the chiller operative condition are concerned, they are listed in Table 3.

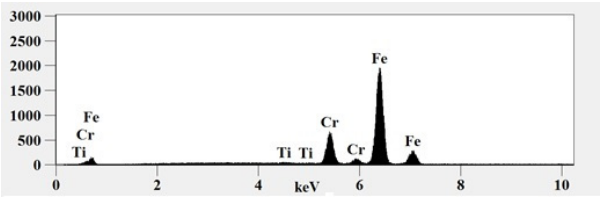


Fig. 2. EDS spectrum showing the stainless steel composition.

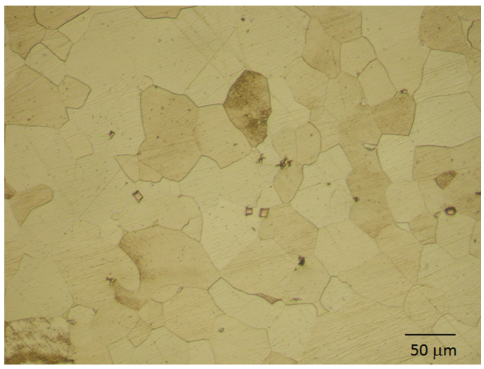


Fig. 3. Optical micrograph showing the stainless steel microstructure.

Table 2. Chemical composition (%) of the stainless steel pipes used in the generator

| Fe | C | Si | Mn | P | S | Cr | Ni | Ti | V |
|---|---|---|---|---|---|---|---|---|---|
| Bal. | 0.08 | 0.25 | 0.46 | 0.08 | 0.05 | 17.2 | 0.17 | 0.37 | 0.16 |

The studied failure evolved in two steps. The first step involved the failure of the water copper pipelines and happened after few months from the plant start up.

Before being put into service, the chiller was held for about a year outdoors, near the sea. During this time the chiller lost the nitrogen protection overpressure and the coupling flanges between chiller and chilled water / cooling water circuits remained open. This allowed the input of pollutants and corrosive compounds into the pipelines. After few months from the system start up there was a leakage of water from the chilled water circuit that diluted the LiBr solution and produced a loss of the vacuum inside the chiller. The failed pipe has been excluded from the circuit and the chiller has been restarted. Shortly afterwards there was another water leakage from the pipelines with consequent dilution of the LiBr solution. The chiller has been stopped in order to identify the causes of corrosion and the possible solutions. The failure analysis has been carried out not only on the pipe of the chilled water circuit, but also on those of the cooling water circuit and of the condenser. Once the study has been carried out, failed copper pipes have been replaced and the chiller has been restarted.

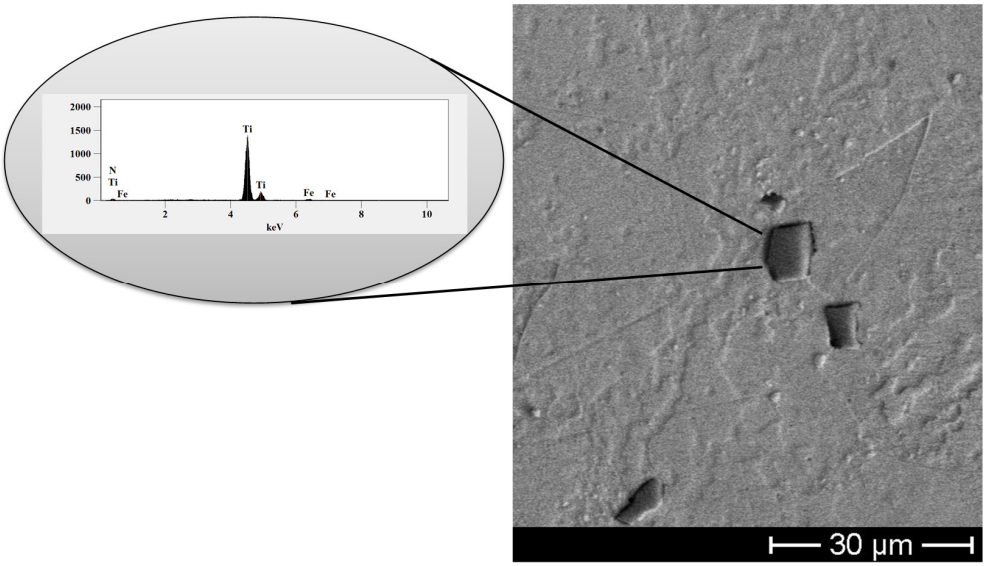


Fig. 4. SEM micrograph showing Ti nitride particles present in the steel matrix.

The second failure step involved the stainless steel pipelines present in the generator section and happened just few months after the chiller restart. The hot water leakage diluted the LiBr solution. The plant has been stopped and failed pipes have been removed in order to be analyzed.

Table 3. Operative conditions of the absorption chiller.

| Parameters | Value |
|---|---|
| Ambient temperature | 5-45 °C |
| Maximum pressure in chilled water lines | 7.7 MPa |
| Inlet chilled water temperature | 6.7 °C |
| Outlet chilled water temperature | 12.7 °C |
| Minimum chilled water temperature | 4.5°C |
| Number of pass in the evaporator | 4 |
| Pressure in the shell (evaporator/absorber) | 8 10-4 MPa |
| Flesh temperature of water inside the shell | 3.7 °C |
| Maximum pressure in cooled water lines | 7.7 MPa |
| Inlet cooled water temperature | 29.4 °C |
| Outlet cooled water temperature | 36.8 °C |
| Number of pass in the absorber | 2 |
| Number of pass in the condenser | 1 |
| Minimum operating cooling water temperature | 20 °C |
| Maximum pressure in hot water lines | 4.8 MPa |
| Inlet cooled water temperature | 96.5 °C |
| Outlet cooled water temperature | 85 °C |
| Number of pass in the generator | 2 |
| LiBr concentration | >60 %, < 70% |

## 3. Failure analysis

### *3.1. First step (failure of copper pipes)*

As already said, the first step of the failure involved the copper pipes present inside the chiller. Their failure produced the loss of the vacuum in the vessel and the LiBr solution dilution. Both corrugated and mini finned pipes have been removed in order to identify the failure position and the possible causes. Some copper pipes employed in the condenser have been also removed in order to verify if they too were affected by corrosion.

Fig. 5 shows the appearance of the external surface of copper pipes. It can be noticed that all pipes are covered by a black oxidized patina. Macrographs have been taken in correspondence of the sections where the copper pipes are in contact with the steel (C40) supports. Fig. 5a shows the surface of the copper plain pipe used in the condenser. On this surface the water vapor produced in the generator condenses. Fig. 5b shows the surface of the copper mini finned pipe employed in the absorber section. On this surface the LiBr solution, which heats up when it absorbs the water vapor produced in the evaporator section, is cooled down. It can be noticed again that in correspondence of the support a corrosion scale is developed. Fig. 5c shows the surface of the copper corrugated pipe employed in the evaporator section. The water flowing inside it, is cooled down from the flashing water that comes from the condenser. A close observation of its surface highlights that also in this case a corrosion scale is formed in the contact points between the pipe and the supports.

The presence of these corrosion products initially suggested that the failure of the pipes could be due to the galvanic coupling between the steel support and the copper pipe and worsened by the development of crevice corrosion.

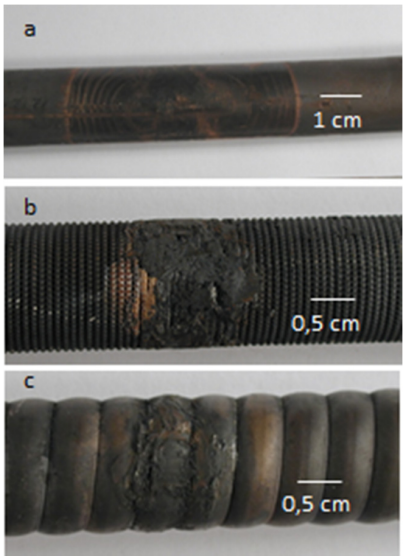


Fig. 5. Macrographs of the external surfaces of copper pipes: a) Condenser, plain pipe, b) Absorber, mini finned pipe, c) Evaporator, corrugated pipe.

In order to verify this hypothesis metallographic analyses have been carried out on specimens taken from those areas. They have been observed by means of a scanning electron microscope (SEM) equipped with energy dispersion spectroscopy (EDS) microanalysis. In addition to this, the corrosion scale has been analyzed by x-ray diffraction. Figs. 6a and c show the surface of the corrugated and mini finned pipes, while Figs. 6b and d show the metallographic transverse sections of specimens taken from the same areas. It can be observed that, at high magnification, the scale is only laid down on the external pipe surfaces, in fact Figs. 6b and d reveal that the profile of the external surfaces of both mini finned and corrugated pipes is almost intact. The scale is localized in correspondence of the supports and its thickness decreases moving away from them. Figs. 7 and 8 show the EDS spectrum and the x-ray diffraction pattern

of the corrosion scale respectively. As it can be seen the corrosion product is iron oxide coming from the corrosion of the steel supports. From this preliminary examination it can be inferred that the failure did not occur in this area.

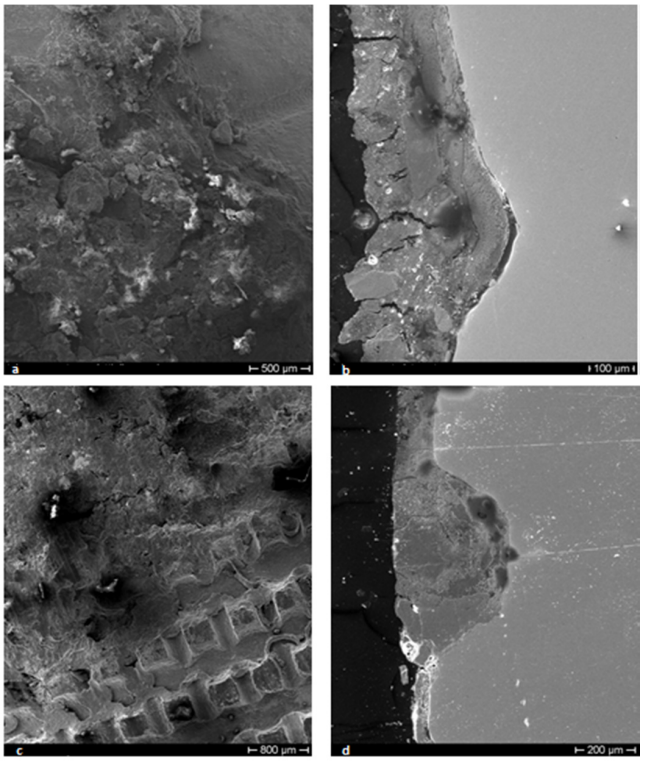


Fig. 6. SEM micrographs of the external surface of copper pipes: Condenser, plain pipe (a, b); Absorber, mini finned pipe (c, d) .

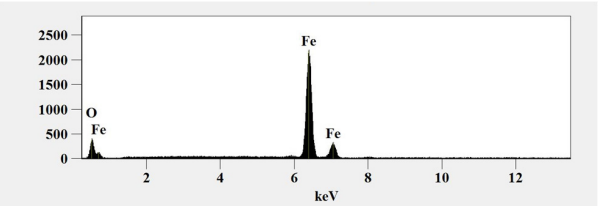


Fig. 7. EDS spectrum of the corrosion scale found in correspondence of the steel supports.

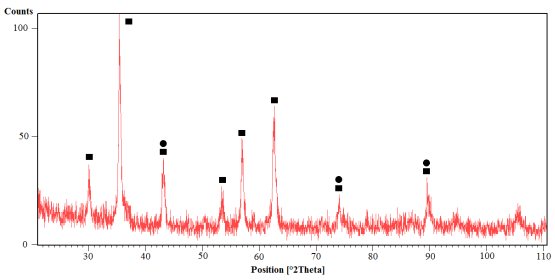


Fig. 8. X-ray diffraction pattern of the corrosion scale found in correspondence of the steel supports (●Cu ■ $Fe_3O_4$).

During the pipes' analyses it has been noticed that the corrugated pipe internal surfaces were completely covered by a green layer, while the other copper pipes were almost clean (Figs. 9 a-c). The green compound has been removed and analyzed by x-ray diffraction, moreover several samples were taken along the whole length of the pipe and the polished cross sections observed by SEM/EDS.

Figs. 10 and 11 show that this green layer was formed by a mixture of iron and copper oxides and by copper bromide hydroxide ($CuBr_2(OH)_3$). SEM observations of the polished cross sections (Fig. 12) revealed that deep corrosion pits developed from the internal surface of the corrugated pipe; in some cases they developed through the whole pipe section. EDS analyses carried on the compounds present inside the pits showed that they were constituted by copper chloride and/or copper bromide hydroxide.

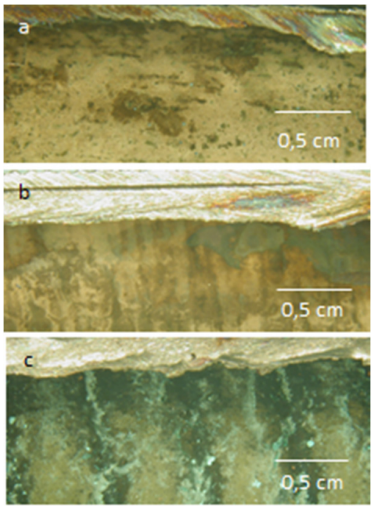


Fig. 9. Macrographs of the internal surfaces of copper pipes: Condenser, plain pipe (a), Absorber, mini finned pipe (b), Evaporator, corrugated pipe (c).

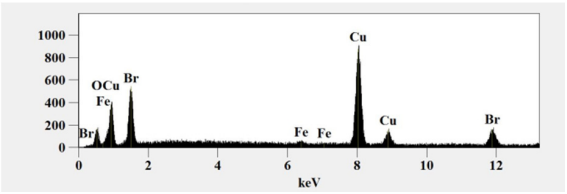


Fig. 10. EDS spectrum of the deposit found inside the corrugated pipe

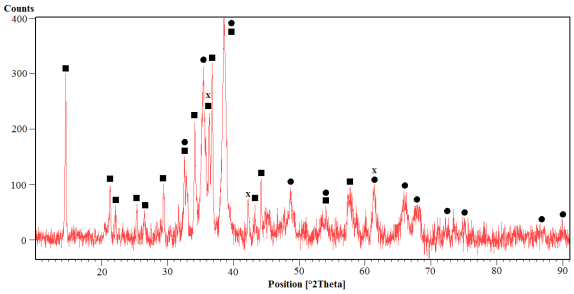


Fig. 11. X-ray diffraction pattern of the deposit found inside the corrugated pipe( ■ $Cu_2$ Br ( O H )$_3$ , ●CuO, X FeO)

SEM observation of the polished cross section of the corrugated pipes showed that these pipes were subjected to a deep localized corrosion attack that started from the internal surface. Fig. 12 shows deep pits that in several cases developed almost through the whole pipe section. These pits are full of corrosion products. The presence of halides inside these pipes was unexpected, in fact chlorine is virtually absent in this plant and only traces of this element could be found in the softened water flowing in the chilled water circuit. However it must be considered that the chiller was stored for about a year near the sea and that during this time span the coupling flanges remained open allowing moisture and chloride to enter the pipes. The occurrence of localized corrosion phenomena has just been noticed after the first plant stop during a visual inspection carried out with an endoscope. It showed the presence of pits inside many copper pipes both in the evaporator and in the absorber sections. Some pipes had also the internal surface covered by a thick layer of a corrosion product deposit. As it can be seen from the plant schema reported in figure 1 bromine should be present only in the absorber zone of the chiller that should be separated by a septa from the evaporator section where the failed corrugated pipes are placed. Bromides can enter the evaporation section only if there is a

sudden increase of the LiBr solution level due to a plant malfunction. This probably happened as a consequence of the first chilled water circuit failure, when pressurized water from this circuit flooded the chiller.

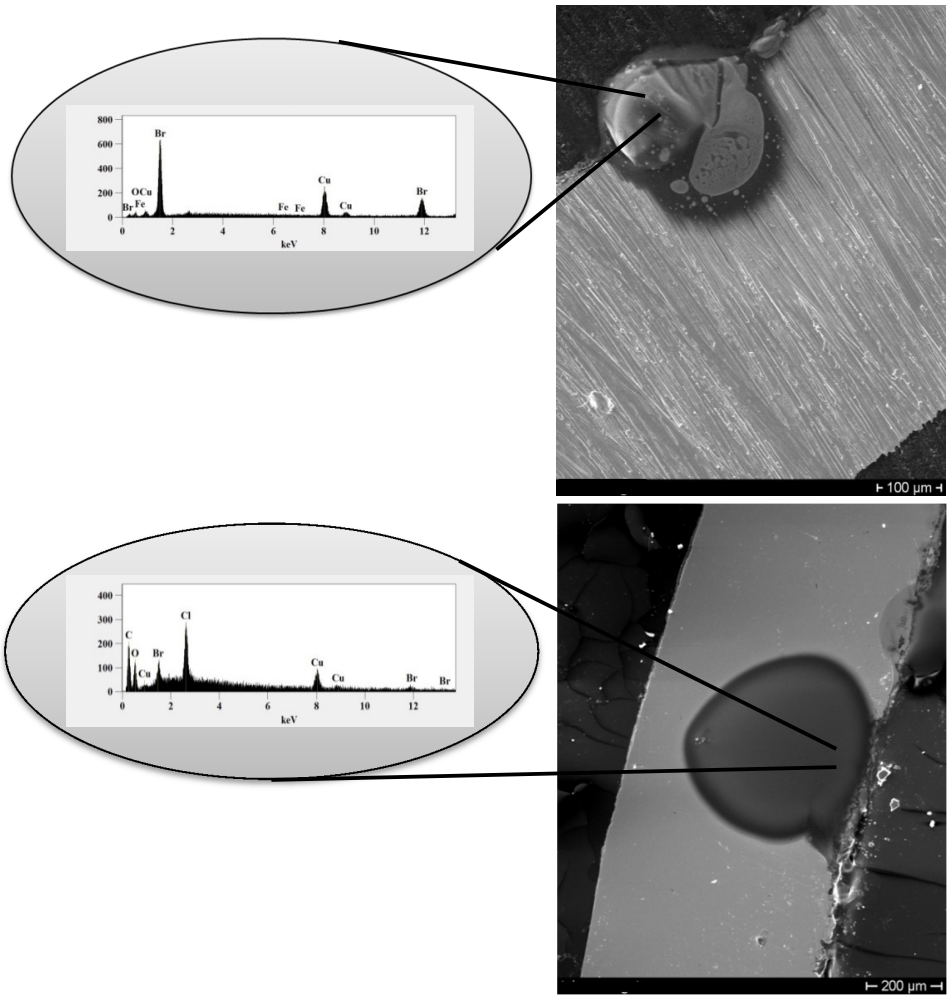


Fig. 12. SEM micrographs showing two deep pits developed in the corrugated copper pipes.

The storage of the chiller in proximity of the sea, where the concentration of chlorides in the air is high, probably creates the conditions for a localized corrosion attack that started form the pipe internal surface. Generally speaking halides generate a very aggressive environment for copper [1-3] that in halide solutions exhibits an active behavior. Chloride ions in fact tend to form soluble chloride complexes ($CuCl_2^-$ and $CuCl_3^{2-}$) that are easily dissolved. The deep pits developed and the high pressure difference between the inside and the outside of the pipes probably caused the first observed failure. The external surfaces of copper pipes were protected because pipes were placed in the closed chiller vessel and kept under inert gas (nitrogen) overpressure.

After the first failure, leak tests were carried out in order to identify the damaged pipes that were then excluded from the circuit. Moreover mini finned copper pipes present in the absorber section have been chemically cleaned with hydrochloric acid. The plant was then restarted, but after few months the copper pipelines failed again. This second failure was caused by old pits and by new pits developed under the bromide layer previously described.

Considering that halide ions behave similarly, bromides also favor localized corrosion phenomena. They are aggravated by the presence of the salt deposit that can favor crevice corrosion initiation and propagation.

Once the causes of failure have been identified all copper pipes were replaced with new ones.

### *3.2. Second step (failure of stainless steel).*

After few months from the chiller restart, some pipes of the hot water circuit in the generator failed causing a new plant downtime. Pipes in the generator, as already said in Section 2, are made of stainless steel. Pressurized hot water flows inside them, while their external surface is in contact with a diluted LiBr solution at a pressure of about 8 $10^{-4}$ MPa. Some failed pipes were removed for a complete metallographic analysis.

A naked eye observation of the corroded pipes revealed that there are defects developing from the internal surfaces through the whole section of the pipes. Figs. 13 a and b show the macrographs of a defect observed on the external and on the internal pipe surface respectively. On the external surface a crevice is clearly visible, while on the internal surface this defect appears as a deep hole surrounded by red corrosion products (iron oxide). In this area several pits have been observed and some of them were rather deep. Figures 14 and 15 show the SEM micrographs of these defects. EDS microanalysis carried out on the metal surface inside the pits show a low oxygen content.

In order to understand the causes of this corrosion phenomenon it must be considered that during a plant inspection, carried out to gather information about the first step of the failure, it was noticed that all the flanges connecting the plant pipelines to the external circuits were open and that there was stagnant water inside all the pipes. This suggested that the failure in the generator could be due to phenomena of differential aeration. The localized corrosion by differential aeration is established when part of a metallic surface is easily reached by oxygen dissolved in water, while another part is not. The oxygen-starved surface become anodic and can be subjected to intense corrosion.

The metal ions dissolved in the anodic region migrate towards the cathodic region where they react with $OH^-$, produced by oxygen reduction, and precipitate as metal hydroxide. This corrosion mechanism produces a deep localized corrosion attack (deep pits) in the oxygen-starving areas while metal hydroxides precipitate close the air-water interface. The generator pipes' analyses showed that these pipes were also subjected to a second type of corrosive attack. Figures 16 a and b show the external surface of stainless steel mini finned pipes which are frequently covered by dark spots. The corresponding internal surfaces were defect free. Figures 17 and 18 show SEM micrographs of the damaged external surface and of the cross sections taken in correspondence of the defects. In the central part of each dark spot a pit was always identified. EDS analyses showed that inside the pits a titanium rich particle is often present and that copper is always detected in the corrosion products surrounding the pits.

This corrosion phenomenon was not responsible for the failure of the generator pipeline because pits were not so deep to perforate the pipes and to produce water leakage. Despite that, causes of pits' formation must be identified because their depth would increase with time and then they could perforate the pipes again. Pits can form on stainless steel components only if the "passive" film that protects the metal surface breaks up locally.

This film breakdown occurs when the potential become higher than the breakdown potential ($E_B$). The $E_B$ value depends on metallurgical and environmental factors. In the case of stainless steel $E_B$ increases with increasing the content of chromium, nickel and molybdenum, but it can be lowered either by the presence of inclusions or of work-hardened zone and wherever the passive film is defective the underlying alloy can start to dissolve locally. $E_B$ value is considerably reduced by the presence in the environment of specific ions such as halogen ions that promote pitting corrosion, which is often the cause of catastrophic failure of metallic components [4-7]. In the presented case study all of the chemical and metallurgical factors that can cause pitting corrosion were present. In fact although pipes are made of a stainless steel with a Cr content (17%) which is able to promote the formation of a protective passive film, the environment surrounding pipes is very rich of halogen ions (LiBr diluted solution). Moreover the microstructure of this stabilized stainless steel is characterized by a massive presence of non metallic inclusions (titanium carbide/nitride particles). Plastic deformation necessary to obtain the mini finning produced work-hardened areas and probably damaged locally the passive film. All of these factors decrease the $E_B$ value making the alloy more prone to pitting corrosion.

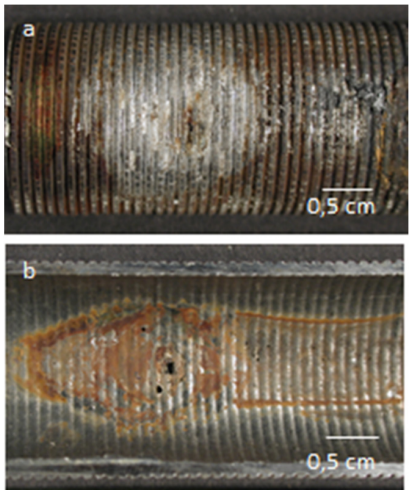


Fig. 13. Macrographs of the stainless steel pipe external (a) and internal (b) surfaces.

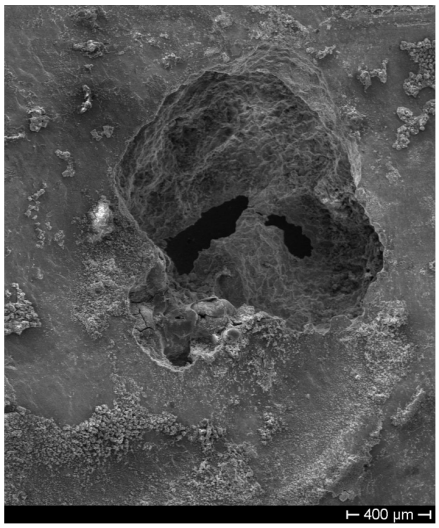


Fig. 14. SEM micrograph showing a deep pit on the surface of the stainless steel pipe.

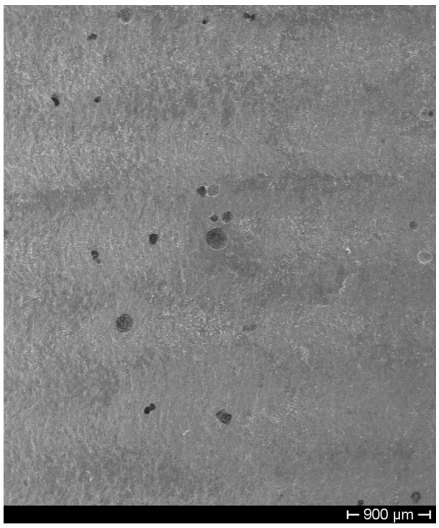


Fig. 15. SEM micrograph showing small pits developed on the internal surface of the stainless steel pipe.

In order to fully understand the corrosion process occurred in the generator, it is necessary to identify the cathodic process. Considering that the generator operates under vacuum and that metallic copper has been found around pits the reduction of cupric ions to metallic copper ($Cu^{2+}+2e^{-} \rightarrow Cu$) is thought to be the most likely cathodic process. In fact copper ions dissolved in the LiBr solution, as consequence of copper pipeline corrosion in the absorber, were carried into the generator where they could be reduced to metallic copper.

As far as the present case study is concerned, the most important factor causing pit initiation and propagation seems to be the presence of titanium carbide inclusions that are always found inside the pits. Studies available in literature [8-11] highlight that non-metallic inclusions promote the formation of defective passive films. For stainless steels sulfide inclusions are primary responsible for pitting initiation, but it has been demonstrated the titanium rich inclusions behave cathodically with respect to both sulfide inclusions and metallic matrix and hence they promote localized attack. That means that titanium stabilized steels are characterized by a low susceptibility to intergranular attack, but a high rate of pitting corrosion.

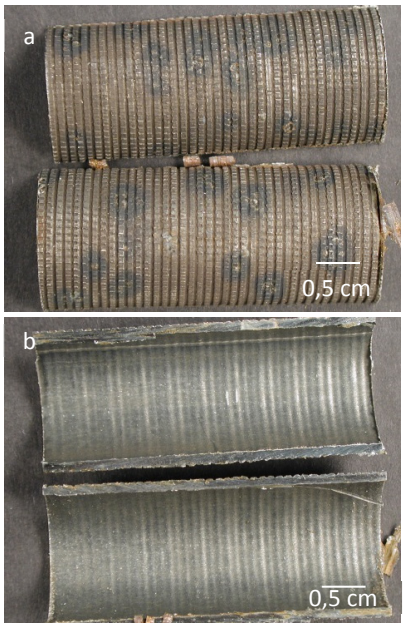


Fig. 16. Macrographs of the stainless steel pipe external (a) and internal (b) surfaces.

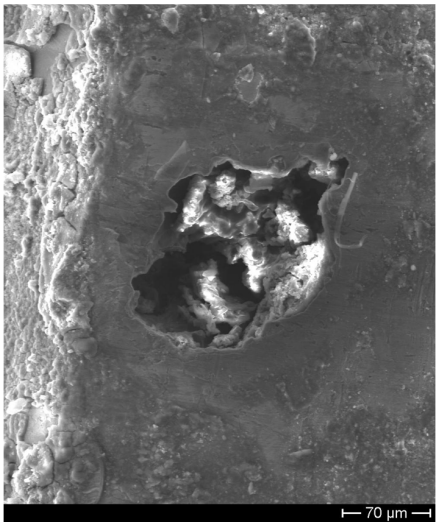


Fig. 17. SEM micrograph of a pit developed on the stainless steel pipe external surface.

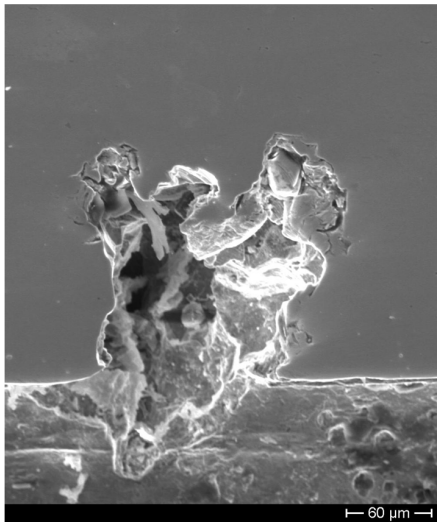


Fig. 18. SEM micrograph of a pit on stainless steel pipe external surface (metallographic section) .

In order to fully understand the corrosion process occurred in the generator, it is necessary to identify the cathodic process. Considering that the generator operates under vacuum and that metallic copper has been found around pits the reduction of cupric ions to metallic copper ($Cu^{2+}+2e^{-} \rightarrow Cu$) is thought to be the most likely cathodic process. In fact copper ions dissolved in the LiBr solution, as consequence of copper pipeline corrosion in the absorber, were carried into the generator where they could be reduced to metallic copper.

As far as the present case study is concerned, the most important factor causing pit initiation and propagation seems to be the presence of titanium carbide inclusions that are always found inside the pits. Studies available in literature [8-11] highlight that non-metallic inclusions promote the formation of defective passive films. For stainless steels sulfide inclusions are primary responsible for pitting initiation, but it has been demonstrated the titanium rich inclusions behave cathodically with respect to both sulfide inclusions and metallic matrix and hence they promote localized attack. That means that titanium stabilized steels are characterized by a low susceptibility to intergranular attack, but a high rate of pitting corrosion.

## 4. Conclusions

The study presented in this paper analyses interconnected corrosion processes that developed in different sections of an absorption chiller and that determined several plant downtimes. Copper pipelines used in the evaporator section were stored for about a year near the sea and were subjected to the formation of narrow and deep pits that perforated the pipes during the plant run. Due to this failure water flooded the absorber section and carried bromides in the evaporator, thus exacerbating the copper pipe corrosion process. Copper dissolved in the lithium bromide solution was brought into the generator section where it behaved cathodically, so favoring pitting attack of titanium stabilized stainless steel pipes.

The analysis of failed components explained the different corrosion processes and avoided further plant downtimes.

## References

[1] C. Deslouis, B. Tribollet, G. Mengoli, M.M. Musiani, Electrochemical behaviour of copper in neutral aerated chloride solution. I. Steady-state investigation, J. Appl. Electrochem. 18 (1988) 374-383.
[2] G. Kear, B.D. Barker, F.C. Walsh, Electrochemical corrosion of unalloyed copper in chloride media-a critical review, Corros. Sci. 46 (2004) 109-135.
[3] M.J. Muñoz-Portero, J. García-Antón, J.L. Guiñón, V. Pérez-Herranz, Corrosion of copper in aqueous lithium bromide concentrated solutions by immersion testing, Corrosion. 62 (2006) 1018-1027.
[4] A.I. Muñoz, J.G. Antón, S.L. Nuévalos, J.L. Guiñon, V.P. Herranz, Corrosion studies of austenitic and duplex stainless steels in aqueous lithium bromide solution at different temperatures, Corros. Sci. 46 (2004) 2955-2974.
[5] C. Cuevas Arteaga, J. Porcayo Calderón, C.F. Campos Sedano, J.A. Rodríguez, Comparison of corrosion resistance of carbon steel and some stainless steels exposed to LiBr-H 2O Solution at low Temperatures International, Journal of Electrochemical Science, 7 (2012) 445-470.
[6] D. Pilone, A. Brotzu, F.Felli, Failure analysis of connecting bolts used for anchoring streetlights of a mountain highway, Eng. Fail. Anal. 48 (2015) 137-143.
[7] M.P. Ryan, D.E. Williams, R.J. Chater, B.M. Hutton, D.S. McPhail, Why stainless steel corrodes, Nature. 415 (2002) 770-774.
[8] S.C. Srivastava, M.B. Ives, Role of titanium in the pitting corrosion of commercial stainless steels, Corrosion. 45 (1989) 488-493.
[9] R. Guo, M.B. Ives, Pitting susceptibility of stainless steels in bromide solutions at elevated temperatures, Corrosion. 46 (1990) 125-129.
[10] R.D. Knutsen, A. Ball, Influence of inclusions on the corrosion behavior of a 12 wt% chromium steel, Corrosion. 47 (1991) 359-368.
[11] L.H. Boulton, A.J. Betts, Corrosion performance of titanium and titanium stabilised stainless steels, Brit. Corros. J. 26 (1991) 287-292.